

CHAPTER VI
POLY(3-HYDROXYBUTYRATE)/MAGNETITE COMPOSITE
NANOFIBERS VIA COMBINING ELECTROSPUNNING TECHNIQUE
WITH THE AMMONIA GAS-ENHANCING *IN SITU* CO-PRECIPIATION
METHOD: PREPARTION AND THEIR POTENTIAL USE IN
BIOMEDICAL APPLICATION

6.1 ABSTRACT

In the present contribution, we report a relatively simple way, where magnetic nanoparticles were incorporated into the electrospun ultrafine fibers of poly(3-hydroxybutyrate) (PHB) by electrospinning technology combining with *in situ* co-precipitation method. According to this approach, we achieve the uniform dispersion of the Fe₃O₄ nanoparticles along the fibrous surface. The formation of Fe₃O₄ nanoparticles on the fiber surface and the particle size and its distribution were investigated by scanning electron microscope (SEM), X-ray diffraction (XRD) and energy dispersive X-ray (EDX). The content of Fe₃O₄ nanoparticles in the composite nanofibers were performed by using thermogravimetric analysis (TGA) technique. The potential used in biomedical application was evaluated by indirect cytotoxicity test, using L929 mouse fibroblast and murine neuroblastoma Neuro 2a cell lines.

(Keywords: Electrospinning; Poly(3-hydroxybutyrate); Magnetite nanoparticles; Cytotoxicity)

6.2 Introduction

Recent advances in nanotechnology have greatly expedited the development of magnetically responsive hybrid material that exhibits the interesting magnetic field-dependent behavior which provides the potential use in a wide range of biomedical application [1-6]. The magnetism property can be produced by incorporating magnetically agents into the polymer matrix. Among the various types of magnetically agents, a black iron oxide particle called magnetite (Fe_3O_4) that exhibits the strongest magnetism of any transition metal oxide [7], has heavily studied due to its biocompatibility and low cytotoxicity with living cells [3,8]. The size of particles plays an important role in the magnetic property [9]. Below approximately 100 nm in diameter, particles of ferromagnetic materials no longer exhibit the cooperative phenomenon of ferromagnetism likely found in the bulk. Instead, such nanoparticles exhibit the superparamagnetic property which no longer exhibits a hysteresis [10]. According to the superparamagnetic behavior, such nanoparticles should also deform in the direction of the gradient of the external magnetic field and no longer show magnetic property without the external magnetic field. These changes in the direction should be completely reversible, since the magnetic moment of particles should relax to their original distributions after removal of magnetic field [2,10].

Various approaches have been performed to incorporate superparamagnetic Fe_3O_4 nanoparticles into nanofibers. Electrospinning is a versatile and effective method for the production of polymeric nanofibers with diameters ranging from a few micrometers down to several hundred nanometers. These electrospun fibrous substrates exhibit several interesting characteristics involve high surface area to mass or volume ratio, a small inter-fibrous pore size with high porosity and vast possibilities for surface functionalization, make electrospun polymeric fibers good candidates for control drug delivery and tissue engineering application [11,12]. In addition, this method has been demonstrated to be a simple way to prepare composite nanofibers by electrospinning the Fe_3O_4 nanoparticles-filled polymer solution. Several studies have shown the possibility to produce composite nanofibers by incorporation of Fe_3O_4 nanoparticles in polymer solutions such as poly(lactic acid)

[13], poly(methyl methacrylate) [14,15], polyaniline [16], poly(ethylene oxide) [10], polyacrylonitrile [17-20], poly(vinyl pyrrolidone) [21,22], Poly(vinylidene fluoride) [23], poly(acrylonitrile-co-acrylic acid) [24], poly(vinyl chloride) [25] and poly(vinyl alcohol) [26-29]. However, this traditional strategy exist some disadvantages such as stepwise process and the agglomeration of particles due to the strong Van der Waals force, making the difficulty to re-disperse well in the spinning solution, that can be minimized by coating their surface with steric stabilizers or adsorbing on their surface with surfactants to prevent the agglomeration of neighboring particles [10,29,30].

In the present contribution, we present a novel approach to prepare poly(3-hydroxybutyrate) (PHB) composite nanofibers via combining electrospinning technique with the ammonia gas-enhancing *in situ* co-precipitation method. PHB is a biodegradable and biocompatible thermoplastic polyester produced by various microorganisms that completely degrades to release a normal component of blood and tissue, d,l- β -hydroxybutyrate (HB) [31]. These outstanding properties render PHB good candidates for biomedical application. The as-prepared solution properties and the morphology of the obtained PHB-Fe₃O₄ composite nanofibers were characterized. The existence of Fe₃O₄ nanoparticles and the magnetic properties of PHB-Fe₃O₄ composite nanofibers were also performed. The potential for use of these composite fiber mats as scaffolding materials was evaluated *in vitro* with mouse fibroblasts (L929) and murine neuroblastoma (Neuro2a), in which the indirect cytotoxicity were analyzed. Comparison was made against the tissue-culture polystyrene (TCPS) plates and the pristine as-spun PHB fiber mats.

6.3 Experimental

6.3.1 Materials

Materials used in the fabrication of the PHB-Fe₃O₄ composite nanofibers included poly(3-hydroxybutyrate) (PHB; $M_w = 300,000 \text{ g}\cdot\text{mol}^{-1}$; Sigma-Aldrich, USA), poly(ethylene oxide) (PEO; $M_w = 600,000 \text{ g}\cdot\text{mol}^{-1}$; Acros Organics, Thailand), iron (III) chloride hexahydrate (Honeywell Riedel-de Haën®, Germany),

iron (II) chloride tetrahydrate (Honeywell Riedel-de Haën®, Germany) and 30 wt% ammonia (Lab-scan, Asia). Chloroform (Lab-scan, Asia) and distilled water was used as the solvent. Distilled water was deoxygenated by bubbling nitrogen gas prior to use. All chemicals were used directly without further purification.

6.3.2 Preparation of Spinning Solutions and Electrospinning Experiment

The electrospun PHB-Fe₃O₄ composite nanofibers were fabricated by using electrospinning technique combination with the ammonia gas-enhancing *in situ* co-precipitation method as summarized in Figure 6.1. Briefly, 20% w/v PHB was dissolved in chloroform and stirred for 4 h at 60 °C and 1% w/v aqueous deoxygenated PEO solution containing iron ion was prepared by dissolving the various amounts of iron ion (Fe³⁺ and Fe²⁺ with a fixed ratio at 2:1) into PEO solution and stirred for 6 h at 60 °C to form the hybrid solutions. The total concentration of aqueous iron ion solutions was varied to be 0.05 M, 0.10 M, 0.20 M and 0.30 M. When completely dissolved, the hybrid solutions were mixed into PHB solution with the weight ratio of 1:9 to obtain the as-prepared spinning solutions and stirred vigorously overnight at 60 °C under nitrogen atmosphere. Each of the spinning dopes was subsequently contained in a 20-ml glass syringe, the open end of which was connected to a gauge 20 stainless steel needle (OD= 0.91mm), used as the nozzle. A rotating drum (width and OD of the drum ≈ 15 cm; rotational speed = 200 rpm) was used as a collector. The outer surface of the rotating drum was covered with an aluminum sheet and set about 20 cm from the tip of the needle. A Gamma High Voltage Research DES30PN/M692 power supply was used to generate a fixed dc potential of 15 kV. The collection time was also fixed at about 4 h.

Fe₃O₄ nanoparticles were synthesized into the as-spun PHB nanofibers by using the ammonia gas-enhancing *in situ* co-precipitation method. Briefly, the electrospun PHB containing iron ion were kept inside the reaction vessel and pre-treated with nitrogen gas for 10 min in order to eliminate oxygen gas in the porous fibers. Then, the fiber mats were subsequently exposed in the ammonia atmosphere for 10 min to start the formation of Fe₃O₄ nanoparticles, caused the color of fiber mats gradually changed from yellow to dark brown. The electrospun PHB-Fe₃O₄ composite nanofibers were rinsed successively with distilled water to remove the

residue ammonia until neutral. Finally, the composite fiber mats were dried in vacuo and kept in desiccator prior to further investigation.

6.3.3 Characterization

Prior to electrospinning, each of the spinning solutions was characterized for their viscosity and conductivity using a Brookfield DV-III programmable viscometer and an Orion 160 conductivity meter, respectively. The morphological appearance of the as-spun fiber mats before and after ammonia gas treatment was observed by using a JEOL JSM-5200 scanning electron microscope (SEM) with inbuilt energy dispersive X-ray analysis (EDX). The formation of Fe₃O₄ nanoparticles was verified by X-ray diffraction (XRD) (Rigaku). The obtained composite nanofibers were scanned from $2\theta = 10^\circ$ to $2\theta = 70^\circ$. The content of Fe₃O₄ nanoparticles in composites was determined by using a thermogravimetric analyzer (Perkin Elmer model TGA7) in the temperature range from 50 to 700 °C with a heating rate of 10 °C/min in nitrogen atmosphere. The magnetic property of electrospun composite nanofibers was evaluated by using a vibrating sample magnetometer (VSM; LakeShore Model 7404). The magnetization versus magnetic field (*M-H* curves or hysteresis loops) was plotted as a function of applied magnetic field (Oe) at room temperatures (300 K).

6.3.4 Biological Compatibility Evaluation

To evaluate the potential for use of the electrospun PHB-Fe₃O₄ composite nanofibers in biomedical application, their biocompatibility in terms of indirect cytotoxicity toward mouse connective tissue fibroblast-like cells (L929) and murine neuroblastoma Neuro 2a cell line (American Type Culture Collection: ATCC) was evaluated *in vitro* in comparison with that of the corresponding pristine electrospun PHB fiber mat and tissue-culture polystyrene plate (TCPS). Mouse connective tissue L929 were cultured as a monolayer in Dulbecco's modified Eagle's medium (DMEM; Sigma-Aldrich), supplemented by 5% fetal bovine serum (FBS; Biochrom AG, Germany), 1% l-glutamine (Invitrogen Corp.), and 1% antibiotic and antimycotic formulation [containing penicillin G sodium, streptomycin sulfate, and amphotericin B (Invitrogen Corp.)]. For murine neuroblastoma Neuro 2a cell line, the cells were cultured as a monolayer in MEM/EBSS medium (HyClone),

supplemented by 10% fetal bovine serum (HyClone), 2 mM L-glutamine (Gibco) and 1X Pen/Strep (Gibco). The cells were incubated at 37 °C in a humidified atmosphere containing 5% CO₂, and the culture medium was replaced once every 2 d. The reference cells from the cultures were trypsinized [0.25% Trypsin-EDTA (Gibco)], and seeded on TCPS.

The indirect cytotoxicity evaluation of electrospun PHB-Fe₃O₄ composite nanofibers was conducted in adaptation from the ISO10993-5 standard test method. First, the extraction media were prepared by immersing the specimens, cut from the composite fiber mats (~7 mm in diameter), in wells of a 96-well TCPS in a serum-free medium (SFM; containing DMEM, 1% L-glutamine, 1% lactalbumin, and 1% antibiotic and antimycotic formulation) and incubated for 1 d, 3 d and 5 d. In the preparation of the reference cells, L929 and Neuro2a cells were seeded in the wells of a 96-well TCPS at a density of 1.0×10^4 cells/well and incubated in 5% SFM to allow cell attachment on the plate. After 24 h, the culture medium was removed and the as-prepared extraction media were added to the wells. The cells were incubated further for 24 h, after which time the number of viable cells was quantified with 3-(4,5-dimethylthiazol-2-yl)-2,5-diphenyltetrazolium bromide (MTT) assay. The viability of the cells that were cultured with fresh SFM was used as the control.

6.3.5 Quantification of Viable Cells by MTT Assay

The MTT assay is the method used to quantify the amount of viable cells on the basis of the reduction of the yellow tetrazolium salt to purple formazan crystals by dehydrogenase enzymes secreted from the mitochondria of metabolically active cells. The amount of purple formazan crystals formed is proportional to the number of viable cells. First, the culture medium of each cultured specimen was removed and replaced with 100 μL/well of MTT solution (Sigma-Aldrich) at 5 mg·mL⁻¹ for a 96-well TCPS (or 500 μL/well for a 24-well TCPS), and then the plate was incubated for 1 h. After incubation, the MTT solution was removed. Then, 100 μL/well of dimethyl sulfoxide (DMSO; Riedel-de Haën, Germany) was added to dissolve the formazan crystals (or 500 μL/well for a 24-well TCPS), and the plate was left at room temperature in the dark for 1 h on a rotary shaker. Finally, the

absorbance at 570 nm, representing the proportion of viable cells, was recorded by a Thermo Labsystems (Multiscan Ex) spectrophotometer.

6.4 Results and Discussion

Composite nanofibers containing Fe_3O_4 nanoparticles embedded into a polymer are of particular interest in the field of biotechnology and medicine due to their magnetic field dependent physical properties. Among the fibers fabrication technique, electrospinning is a versatile and effective method to prepare fibers with diameters ranging from micrometer down to a few nanometers or more with a simple way to incorporate the nanoparticles into the polymer matrix. However, the major difficulty in preparation of such composite nanofibers is the ability to perform stable dispersion of nanoparticles in the continuous polymer matrix. Here, we report a novel approach where Fe_3O_4 nanoparticles were embedded into the composite nanofibers via combining electrospinning technology with the ammonia gas-enhancing *in situ* co-precipitation method.

6.4.1 Preparation and Characterization of Electrospun Containing Iron Ion and the Obtained Electrospun PHB- Fe_3O_4 Composite Nanofibers

It is a common knowledge that the properties of the spinning solutions play an importance role in the morphological appearance of the obtained electrospun nanofibers. The presence of iron ion in the as-prepared solutions caused the significantly changed in the conductivity and viscosity as shown in Figure 6.2. For a given polymer concentration, the viscosity of solution decreased whereas the conductivity increased with the addition and increasing concentration of the iron ion. These results indicated the strongly effect of added iron ion on the solution properties for producing electrospun nanofibers. Table 6.1 shows selected SEM images of the electrospun pristine PHB and electrospun PHB containing iron ion nanofibers that were produced under a constant electrical potential and over a fixed collection distance. Evidently, the addition of iron ion resulted in the formation of smaller fibers, in comparison with those obtained from the pristine PHB solution. The fiber diameters decreased gradually from $2.68 \pm 0.79 \mu\text{m}$ of pristine PHB to 2.16 ± 0.68

μm and $1.31 \pm 0.53 \mu\text{m}$ with the increasing iron ion concentration up to about 0.05 M and 0.10 M, respectively. When the concentration of aqueous iron ion solution increased up to 0.20 M, the fiber diameters also decreased to $0.68 \pm 0.29 \mu\text{m}$ with a combination of beaded fibers was observed. At concentration greater than 0.30 M of aqueous iron ion solution, electrospinning of such solutions resulted only in the formation of discrete beads (data not shown). The increasing in the solution conductivity and the decreasing in the solution viscosity contribute to the observed decrease in the fiber diameter and ability to form continuous fibers due to the Coulombic repulsion of charges present within the jet segment and the less mechanical resistance when the fibers undergoing bending instability [31]. In case of bead formation, the degree of chain entanglement is not high enough to withstand the Coulombic stretching force acting on the jet segment, causing the jet to break up into smaller jets that are later rounded up to form beads [32]. For further study, the as-prepared solution of pristine PHB and PHB containing iron ion were electrospun continuously for 4 h to produce the as-spun fiber mats with thickness of about $192 \pm 25 \mu\text{m}$. The as-spun fibers containing iron ion had the yellow surface that resulted from the incorporation of iron ion. After the ammonia gas treatment, the color of as-spun fibers containing iron ion changed from yellow to dark brown which indicated the formation of Fe_3O_4 nanoparticles in the composite nanofibers.

The formation of Fe_3O_4 nanoparticles in the PHB- Fe_3O_4 composite nanofibers was confirmed by X-ray diffraction (XRD) analysis and the diffraction patterns are presented in Figure 6.3. From the literature [24], the characteristic diffraction patterns of pure Fe_3O_4 crystals are observed at $2\theta = 30.40^\circ, 35.81^\circ, 43.53^\circ, 54.02^\circ, 57.59^\circ$ and 63.25° corresponded to (2 2 0), (3 1 1), (4 0 0), (4 2 2), (5 1 1) and (4 4 0) planes, respectively. For the electrospun pristine PHB fiber mat, the characteristic diffraction pattern peak was observed at $2\theta = 12.4^\circ, 16^\circ, 20^\circ$ and 23° , which corresponding to the diffraction patterns of the crystalline PHB polymer powder [33]. All the diffraction patterns of the obtained electrospun PHB- Fe_3O_4 composite nanofibers were observed, which were in agreement with the characteristic XRD patterns of pure Fe_3O_4 nanoparticles, indicating that Fe_3O_4 nanoparticles were formed after the ammonia gas treatment. However, the peak

intensity of Fe_3O_4 nanoparticles decreases and full width of the peak increases, which indicates the low crystallinity and small crystallite size. These results might be predominantly attributed to the existence of the polymer matrix decreased the ability to form Fe_3O_4 nanoparticles, caused the decreasing in the crystal size and crystallinity of nanoparticles [28].

Table 6.1 shows selected SEM images of the electrospun PHB- Fe_3O_4 composite nanofibers using 0.05 M, 0.10 M and 0.20 M of aqueous iron ion solutions. This result show the regular shapes of the Fe_3O_4 nanoparticles distributed uniformly along the fibrous surface. The distribution of Fe_3O_4 nanoparticles on the fiber surface might be a result of the local electric field from electrospinning process [10]. The average particle size of Fe_3O_4 nanoparticles that distributed on the fiber surfaces were about 67.62 ± 15.40 nm, 75.33 ± 21.39 nm and 82.81 ± 25.74 nm for 0.05 M, 0.10 M and 0.20 M of aqueous iron ion concentrations, respectively. The increase in the average particle size with increasing concentration of the aqueous iron ion solution has been also reported by Deepa *et al.* [34]. The existence of Fe_3O_4 nanoparticles throughout the fibers were also confirmed by energy dispersive x-ray (EDX) analysis. Figure 6.4 show EDX analysis of the composite nanofibers using 0.10 M of aqueous iron ion solution. Several strong peaks at 0.7 eV, 6.4 eV and 7.1 eV representative of Fe can be observed. This result indicated that Fe_3O_4 nanoparticles also exist in the surface layer of the electrospun composite nanofibers.

The content of Fe_3O_4 nanoparticles incorporated in the composite nanofibers was further examined by thermogravimetric analysis (TGA). To avoid the possibility of weight increase as a result of iron oxidation and to allow the thermal decomposition of the polymer, these analyses were performed under nitrogen atmosphere. The pristine PHB fiber mats exhibited only one stage decomposition started from ~ 200 °C to 280 °C due to the breakdown of the polymer backbone without some residues. For the fibrous composites, the TGA thermogram exhibited a two stage decomposition of which the one observed up to ~ 120 °C was due to the removal of adsorbed moisture which corresponded to ca. 3% weight loss. The second step decomposition that corresponded to the degradation of polymer matrix was also observed. Remaining weight of the residues was presented, as a result of the Fe_3O_4

nanoparticles. The theoretical amount of Fe_3O_4 nanoparticles could be created by a given amount of iron ion reactants were calculated to be 16.46 wt.%, 27.64 wt.% and 36.53 wt.% for the iron ion concentration of 0.05 M, 0.10 M and 0.20 M, respectively. However, the practical amount of Fe_3O_4 nanoparticles in the fibrous composite that estimated from the residual mass percentages were about 2.5 wt.%, 6 wt.% and 11 wt.% as shown in Figure 6.5, respectively. The significantly difference in the amount of Fe_3O_4 nanoparticles between the theoretical and practical contents might be predominantly attributed to the hindering of the growth of nanoparticles due to the existence of the polymer matrix which affects the ability to form nanoparticles.

The superparamagnetic behavior of the electrospun PHB- Fe_3O_4 composite nanofibers at room temperature is especially useful for application in nonuniform magnetic fields due to the ability to significantly reduce the dissipative energy in the devices. The magnetic hysteresis curves of the composite nanofibers show superparamagnetic behavior with a symmetric hysteresis and saturation magnetization at room temperature as is evident in Figure 6.6. With the decreasing of the magnetic field, the magnetization decreased and reaches zero with a small remnant magnetization. The saturation magnetization (M_s) of composite nanofibers were $0.13 \text{ emu}\cdot\text{g}^{-1}$, $0.44 \text{ emu}\cdot\text{g}^{-1}$ and $0.60 \text{ emu}\cdot\text{g}^{-1}$ for 0.05 M, 0.10 M and 0.20 M of aqueous iron ion solutions, respectively. However, the magnetization of the bulk Fe_3O_4 from the literature was $90 \text{ emu}\cdot\text{g}^{-1}$ [35]. The decrease in magnetization of the electrospun PHB- Fe_3O_4 composite nanofibers is attributed to the follow reasons: (1) the existence of polymer matrixes that encapsulated Fe_3O_4 nanoparticles affect the magnetization expression of the Fe_3O_4 nanoparticles [28]; (2) the small particle size diameter, results in the reduction of magnetic moment in such nanoparticles [9]. To achieve the superparamagnetic properties, the remnant magnetization (M_r) and the coercive field (H_c) of the electrospun PHB- Fe_3O_4 composite nanofibers should be as low as possible. The remnant magnetizations of composite nanofibers at room temperature were found to be $0.025 \text{ emu}\cdot\text{g}^{-1}$, $0.105 \text{ emu}\cdot\text{g}^{-1}$, and $0.125 \text{ emu}\cdot\text{g}^{-1}$ whereas the coercive fields were found to be 12.53 G, 15.31 G and 17.87 G for 0.05 M, 0.10 M and 0.20 M of aqueous iron ion solution, respectively.

6.4.2 Biological Compatibility Evaluation

To evaluate the potential for use of the electrospun PHB-Fe₃O₄ composite nanofibers in biomedical application, their biocompatibility in terms of indirect cytotoxicity toward mouse connective tissue fibroblast-like cells (L929) and murine neuroblastoma Neuro2a cell line (American Type Culture Collection: ATCC) was evaluated *in vitro* in comparison with that of the corresponding electrospun pristine PHB and tissue-culture polystyrene plate (TCPS). Cytotoxicity is a basic property of scaffolding materials. Figure 6.7 shows the viability of the cells obtained from MTT assay after the cells had been cultured with extraction media from electrospun pristine PHB fiber mats and PHB-Fe₃O₄ composite nanofibers mats as compared with that obtained after the cells had been cultured with the fresh SFM. The viability of the cells was reported as the percentage with respect to that of the control. Evidently, the viability of L929 and Neuro2a cultured with the extraction media from all of fibrous scaffolds were equivalent to that of the cells cultured with fresh SFM. This indicated that the composite nanofibers do not release some cytotoxic substance to the culture media, implying the biocompatibility of these materials toward L929 and Neuro2a. Previous reports showed that Fe₃O₄ nanoparticles had been repeatedly demonstrated with a good biodegradability and without cytotoxicity *in vitro* and *in vivo* [1-4] Results from this work confirmed that the PHB-Fe₃O₄ composite nanofibers obtained from the studied can be serve as ideal candidates for biomedical application.

6.5 Conclusions

In this study, we have successfully prepared the PHB-Fe₃O₄ composite nanofibers by combining electrospinning technology with *in situ* co-precipitation method. The Fe₃O₄ nanoparticles can be in-situ synthesized and well dispersed on the fibrous surface. The average particle sizes of the Fe₃O₄ nanoparticles were in the range of 67-82 nm. The particle size and particle size distribution of Fe₃O₄ nanoparticles were controllable by adjusting the concentration of aqueous iron ion solution. The obtained composite nanofibers have superparamagnetic properties with the saturation magnetization ranged from 0.13 to 0.60 emu·g⁻¹ with very low

remnant magnetization ($0.025\text{-}0.125\text{ emu}\cdot\text{g}^{-1}$) and coercive fields (12-17 G) at room temperature. The potential for use of the obtained composite nanofibers as scaffolding materials for skin and nerve regeneration was further assessed with L929 and Neuro2a in terms of cytotoxicity after they were cultured in the extract media for different of immersion. The viability of L929 and Neuro2a cultured with the extraction media from all of composite nanofiber mats were equivalent to that of the cells cultured with fresh SFM. These results indicate that the PHB-Fe₃O₄ composite nanofibers can be served as ideal candidates for biomedical applications.

6.6 Acknowledgements

This work was supported in part by (1) the Ratchadaphisek Somphot Endowment Fund for Research and Research Unit, Chulalongkorn University and (2) the Center for Petroleum, Petrochemicals and Advanced Materials (CPPAM). P. Sangsanoh thanks a doctoral scholarship (PHD/0191/2550) received from the Royal Golden Jubilee Ph.D. Program, the Thailand Research Fund (TRF).

6.7 References

- [1] Ito, A.; Shinkai, M.; Honda, H.; Kobayashi, T. Medical application of functionalized magnetic nanoparticles, *J Biosci Bioeng* **2005**, 100, 1–11.
- [2] Neuberger, T.; Schopf, B.; Hofmann, H.; Hofmann, M.; Rechenberg, B. Superparamagnetic nanoparticles for biomedical applications: Possibilities and limitations of a new drug delivery system, *J Magn Magn Mat* **2005**, 293, 483–496.
- [3] Tartaj, P.; Morales, M.D.; Veintemillas-Verdaguer, S.; Gonzalez-Carreno, T.; Serna, C.J. The preparation of magnetic nanoparticles for applications in biomedicine. *J Phys D: Appl Phys* **2003**, 36, R182–197.
- [4] Berry, C.C.; Curtis, A.S.G. Functionalisation of magnetic nanoparticles for applications in biomedicine, *J Phys D: Appl Phys* **2003**, 36, R198–206.

- [5] Bajpai, A.K.; Gupta, R. Magnetically mediated release of ciprofloxacin from polyvinyl alcohol based superparamagnetic nanocomposites, *J Mater Sci Mater Med* **2011**, 22, 357-369.
- [6] Hu, S.H.; Liu, T.Y.; Tsai, C.H.; Chen, S.Y. Preparation and characterization of magnetic ferroscaffolds for tissue engineering, *J Magn Magn Mat* **2007**, 310, 2871–2873.
- [7] Cornell, R.M.; Schwertmann, U. The iron oxides: structure, properties, reactions, occurrences and uses, Weinheim 2nd ed. *Wiley-VCH* **2003**.
- [8] Kim, J.S.; Yoon, T.J.; Yu, K.N.; Kim, B.G.; Park, S.J.; Kim, H.W.; Lee, K.H.; Park, S.B.; Lee, J.K.; Cho, M.H. Toxicity and tissue distribution of magnetic nanoparticles in mice, *J Toxicol Sci* **2005**, 89, 338–347.
- [9] Wang, Z.L.; Liu, X.J.; Lv, M.F.; Chai, P.; Liu, Y.; Zhou, X.F.; Meng, J. Preparation of One-Dimensional CoFe_2O_4 Nanostructures and Their Magnetic Properties, *J Phys Chem C* **2008**, 112, 15171–15175.
- [10] Wang, M.; Singh, H.; Hatton, T.A.; Rutledge, G.C. Field-responsive superparamagnetic composite nanofibers by electrospinning, *Polymer* **2004**, 45, 5505–5514.
- [11] Supaphol, P.; Suwantong, O.; Sangsanoh, P.; Srinivasan, S.; Jayakumar, R.; Nair, S.V. Electrospinning of biocompatible polymers and their potentials in biomedical application, *Adv Polym Sci* **2012**, 246, 213-240.
- [12] Sill, T.J.; von Recum, H.A. Electrospinning: Applications in drug delivery and tissue engineering, *Biomaterials* **2008**, 29, 1989-2006.
- [13] Tan, S.T.; Wendorff, J.H.; Pietzonka, C.; Jia, Z.H.; Wang, G.Q. Biocompatible and biodegradable polymer nanofibers displaying superparamagnetic properties, *Chem Phys Chem* **2005**, 6, 1461-1465.
- [14] Pavan Kumar, V.S.; Jagadeesh Babu, V.; Raghuraman, G.K.; Dhamodharan, R.; Natarajan, T.S. Giant magnetoresistance of Fe_3O_4 -polymethylmethacrylate nanocomposite aligned fibers via electrospinning, *J Appl Phys* **2007**, 101, 114317-114320.
- [15] Zhang, C.C.; Li, X.; Yang, Y.; Wang, C. Polymethylmethacrylate/ Fe_3O_4 composite nanofiber membranes with ultra-low dielectric permittivity, *Appl Phys A* **2009**, 97, 281–285.

- [16] Xiao, Q.; Tan, X.K.; Ji, L.L.; Xue, J. Preparation and characterization of polyaniline/nano-Fe₃O₄ composites via a novel Pickering emulsion route, *Synth Met* **2007**, 157, 784-791.
- [17] Wang, B.; Sun, Y.; Wang, H. Preparation and Properties of Electrospun PAN/Fe₃O₄ Magnetic Nanofibers, *J Appl Polym Sci* **2010**, 115, 1781–1786.
- [18] Bayat, M.; Yang, H.; Ko, F. Electromagnetic properties of electrospun Fe₃O₄/carbon composite nanofibers, *Polymer* **2011**, 52, 1645-1653.
- [19] Zhang, D.; Karki, A.B.; Rutman, D.; Young, D.P.; Wang, A.; Cocke, D.; Ho, T.H.; Guo, Z. Electrospun polyacrylonitrile nanocomposite fibers reinforced with Fe₃O₄ nanoparticles: Fabrication and property analysis, *Polymer* **2009**, 50, 4189–4198.
- [20] Nataraj, S.K.; Kim, B.H.; Cruz, M.D.; Ferraris, J.; Aminabhavi, T.M.; Yang, K.S. Free standing thin webs of porous carbon nanofibers of polyacrylonitrile containing iron-oxide by electrospinning, *Mater Lett* **2009**, 63, 218–220.
- [21] Lin, C.R.; Tsai, T.C.; Chung, M.; Lu, S.Z. Synthesis and characterization of magnetic nanoparticles embedded in polyvinyl pyrrolidone nanofiber film by electrospinning method, *J Appl Phys* **2009**, 105, 07B509-11
- [22] Chung, M.; Tsai, T.C.; Lin, C.R.; Lu, S.Z.; Lin, H.Y.; Tsai, J.H.; Chu, C.C. Uniform Fe₃O₄-pyrrolidone nanofibers thin film. EDSSC, *IEEE International Conference* **2008**, 1-4.
- [23] Venugopal, A.; Russell, S.J. Assembly and characterization of PVDF nanofibrous materials with magnetic properties, *World J Eng* **2010**, 310.
- [24] Guo, J.; Ye, X.; Liu, W.; Wu, Q.; Shen, H.; Shu, K. Preparation and characterization of poly(acrylonitrile-co-acrylic acid) nanofibrous composites with Fe₃O₄ magnetic nanoparticles, *Mater Lett* **2009**, 63, 1326-1328.
- [25] Chiscan, O.; Dumitru, I.; Postolache, P.; Tura, V.; Stancu, A. Electrospun PVC/Fe₃O₄ composite nanofibers for microwave absorption applications, *Mater Lett* **2012**, 68, 251–254.
- [26] Chung, M.; Ho, S.F.; Lin, C.R. Electrospun magnetic thin film. Electron Devices and Solid-State Circuits. EDSSC. *IEEE International Conference* **2007**, 309-311.

- [27] Karim, M.R.; Yeum, J.H. Poly(vinyl alcohol)-Fe₃O₄ nanocomposites prepared by the electrospinning technique, *Soft Mater* **2010**, *8*, 197-206.
- [28] Wang, S.; Wang, C.; Zhang, B.; Sun, Z.; Li, Z.; Jiang, X.; Bai, X. Preparation of Fe₃O₄/PVA nanofibers via combining in-situ composite with electrospinning, *Mater Lett* **2010**, *64*, 9–11.
- [29] Mincheva, R.; Stoilova, O.; Penchev, H.; Ruskov, T.; Spirov, I.; Manolova, N.; Rashkov, I. Synthesis of polymer-stabilized magnetic nanoparticles and fabrication of nanocomposite fibers thereof using electrospinning, *Eur Polym J* **2008**, *44*, 615-627.
- [30] Harris, L.A.; Goff, J.D.; Carmichael, A.R.; Riffle, J.S.; Harburn, J.J.; Pierre, T.G.; Saunders, M. Magnetite nanoparticle dispersions stabilized with triblock copolymers, *Chem Mater* **2003**, *15*, 1367–1377.
- [31] Cheng, S.; Chen, G.Q.; Leski, M.; Zou, B.; Wang, Y.; Wu, Q. The effect of D,L-β-hydroxybutyric acid on cell death and proliferation in L929 cells, *Biomaterials* **2006**, *27*, 3758-3765.
- [32] Mit-uppatham, C.; Nithitanakul, M.; Supaphol, P. Ultrafine electrospun polyamide-6 fibers: Effect of solution conditions on morphology and average fiber diameter, *Macromol Chem Phys* **2004**, *205*, 2327-2338.
- [33] Cyras, V.P.; Soledad, C.M.; Analia, V. Biocomposites based on renewable resource: Acetylated and non acetylated cellulose cardboard coated with polyhydroxybutyrate, *Polymers* **2009**, *50*, 6274-6280.
- [34] Deepa, T.; Palkar, V.R.; Kurup, M.B.; Malik, S.K. Properties of magnetite nanoparticles synthesized through a novel chemical route, *Mater Lett* **2004**, *58*, 2692–2694.
- [35] Kennedy, R.J.; Stampe, P.A. Fe₃O₄ films grown by laser ablation on Si (100) and GaAs (100) substrates with and without MgO buffer layers, *J Phys D: Appl Phys* **1999**, *32*, 16–21.

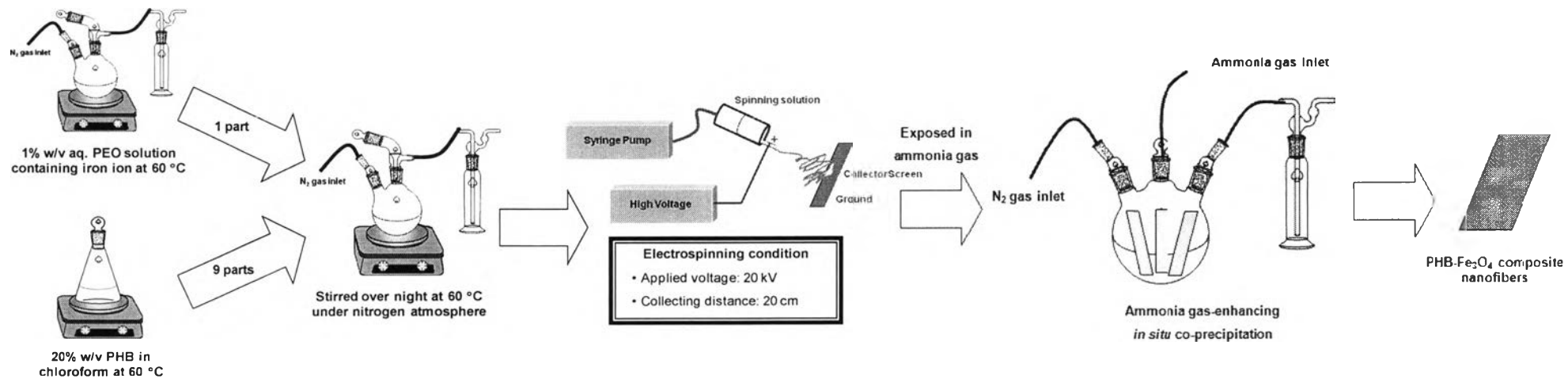


Figure 6.1 Summarizes the pathway for the preparation of PHB-Fe₃O₄ composite nanofibers by using electrospinning technique combination with the ammonia gas-enhancing *in situ* co-precipitation method.

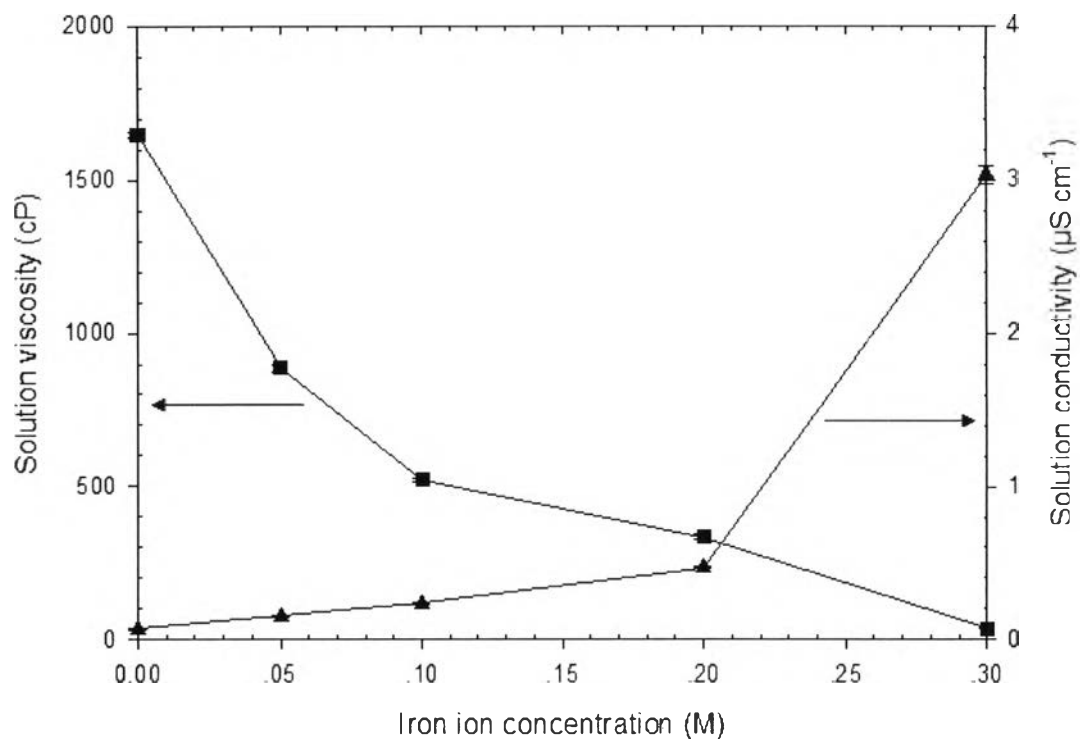


Figure 6.2 Viscosity and conductivity of the as-prepared PHB solution as a function of aqueous iron ion concentration. The as-prepared solution prepared from 20% w/v PHB in chloroform mixed with 1% w/v aqueous deoxygenated PEO solution containing various amounts of iron ion (Fe^{3+} and Fe^{2+} with a fixed ratio at 2:1) with the weight ratio of 1:9.

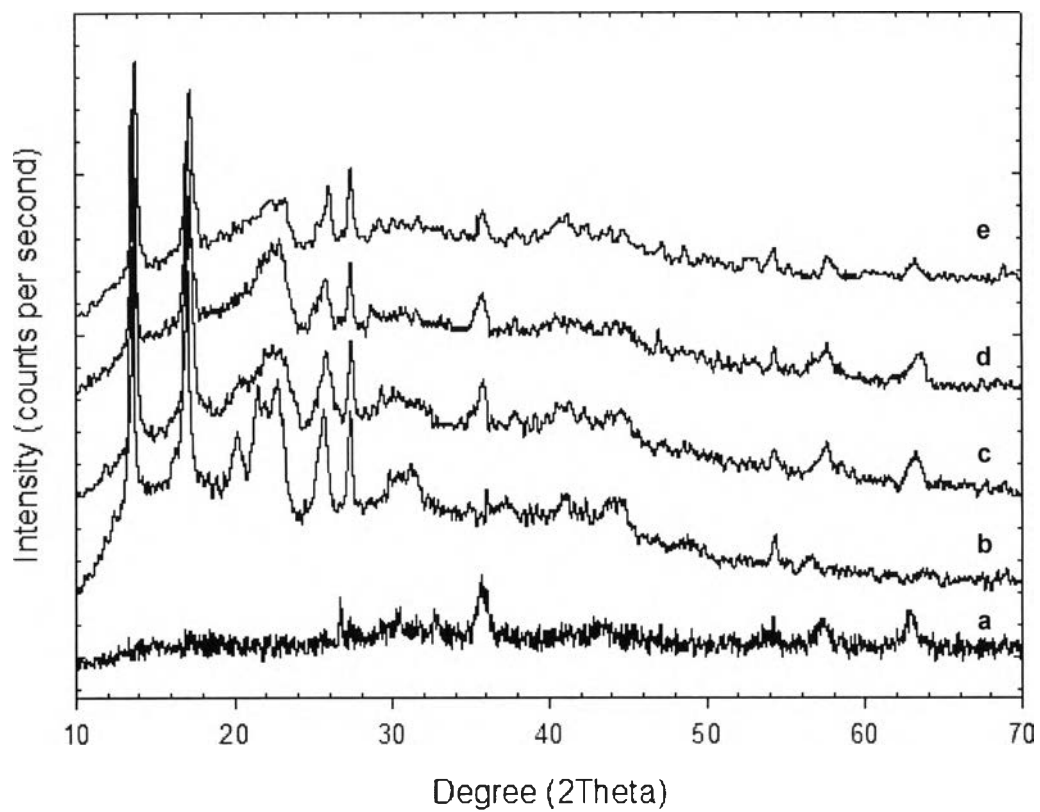


Figure 6.3 Wide-angle X-ray diffraction patterns of Fe_3O_4 nanoparticles (a), pristine PHB (b), PHB- Fe_3O_4 composite nanofibers using 0.05 M (c), 0.10 M (d) and 0.20 M (e) of aqueous iron ion solutions.

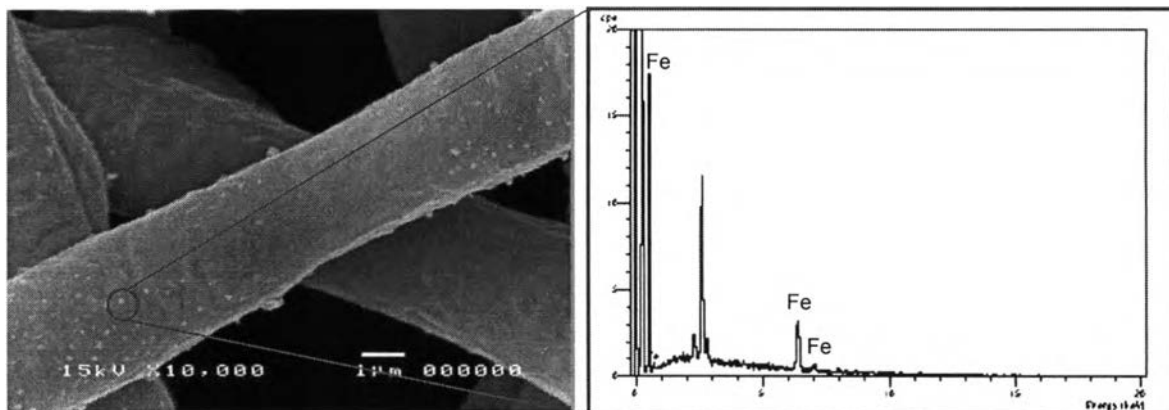


Figure 6.4 The EDX pattern of Fe_3O_4 nanoparticles that presented on the surface of composite nanofibers using 0.10 M of aqueous iron ion solution.

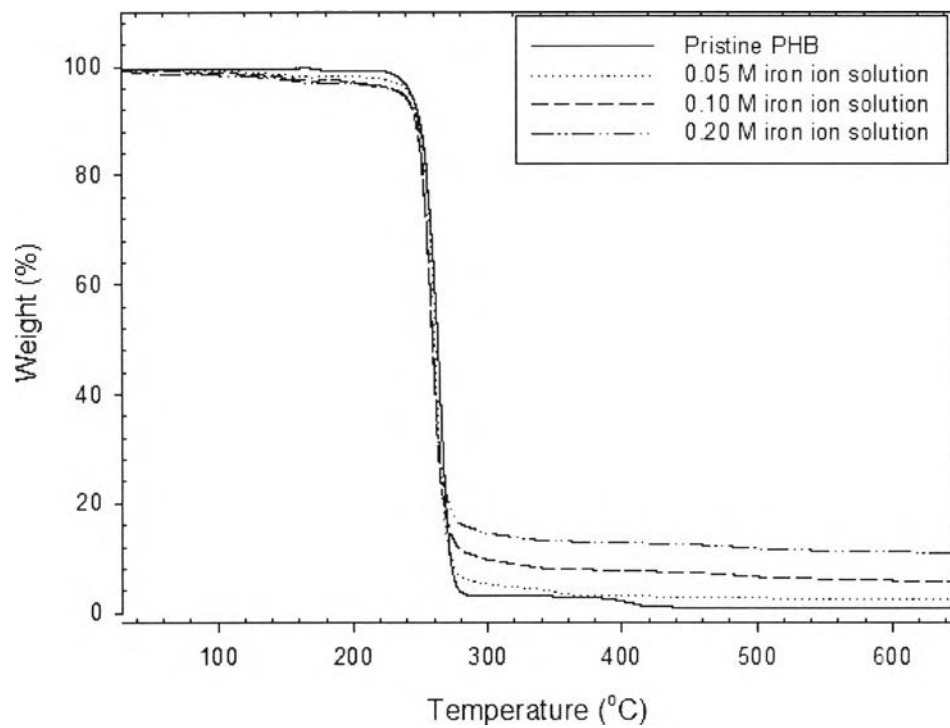


Figure 6.5 TGA thermograms of pristine PHB (a) and PHB-Fe₃O₄ composite nanofibers using 0.05 M (b), 0.10 M (c) and 0.20 M (d) of aqueous iron ion solutions.

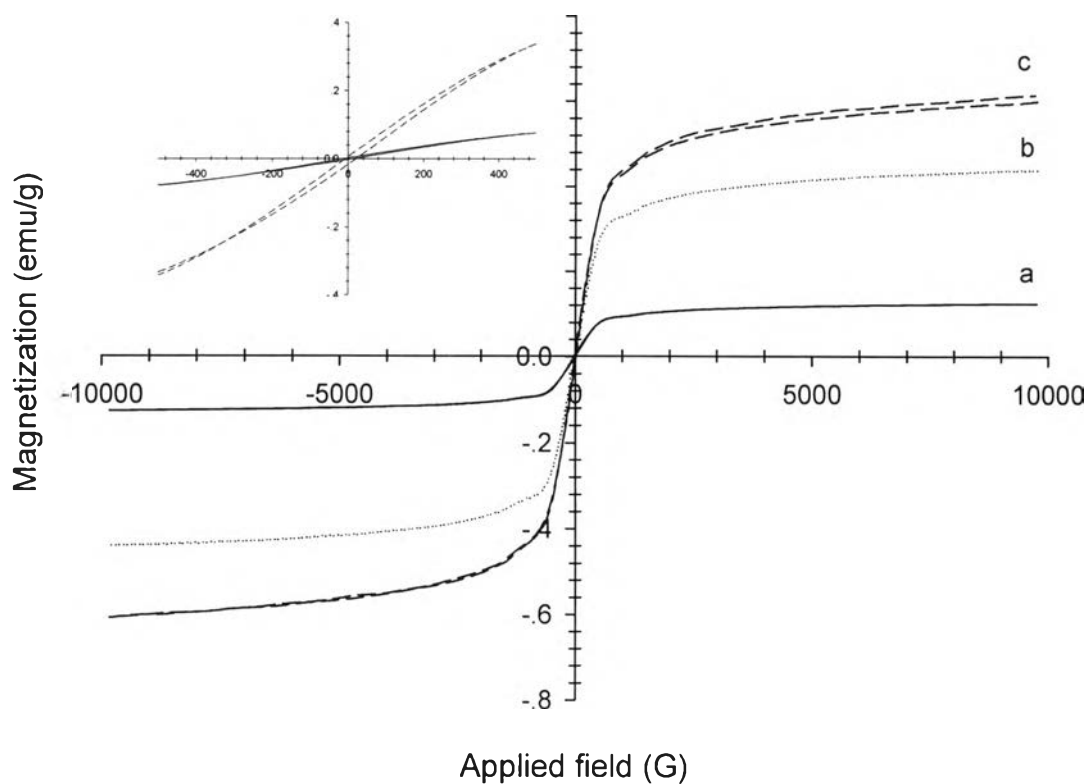


Figure 6.6 Magnetization versus applied magnetic field and magnified view of its hysteresis loop at room temperature of PHB-Fe₃O₄ composite nanofibers using 0.05 M (a), 0.10 M (b) and 0.20 M (c) of aqueous iron ion solutions.

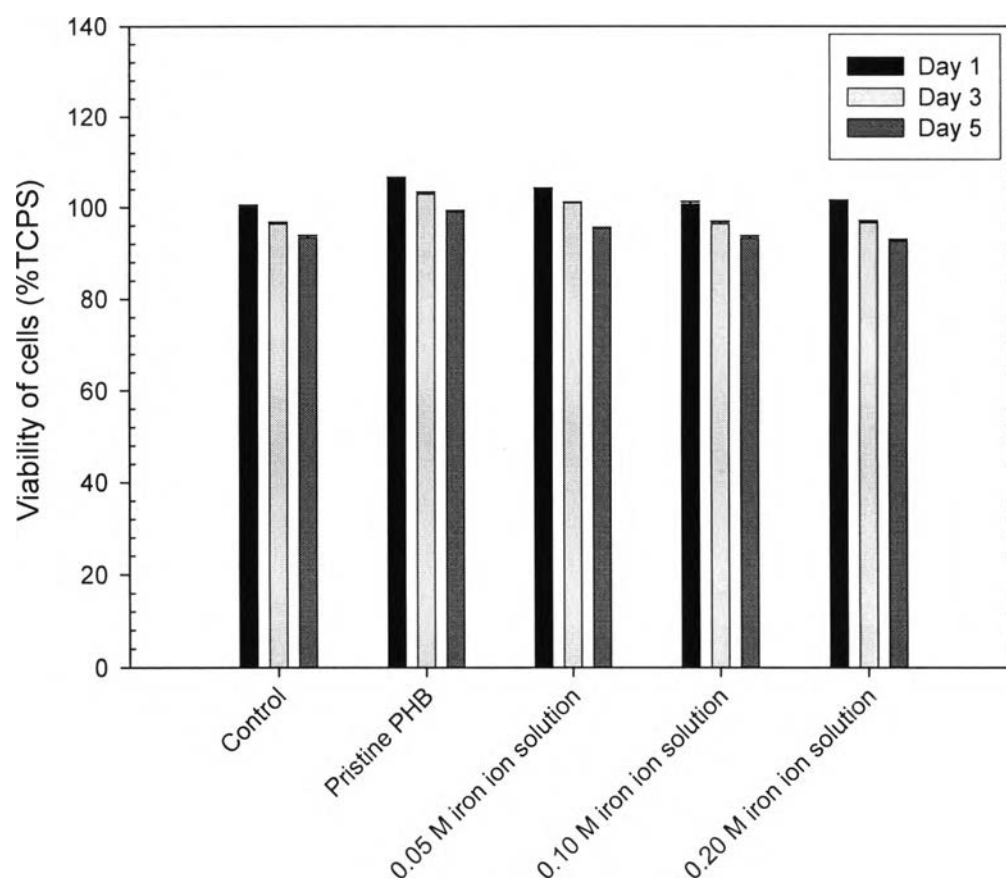
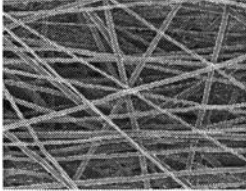
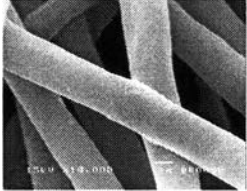
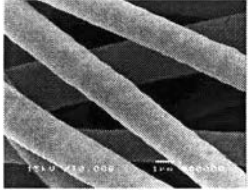
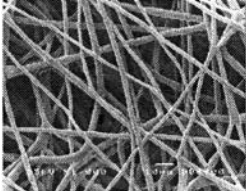
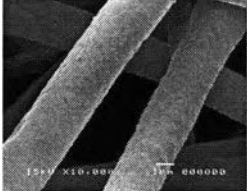
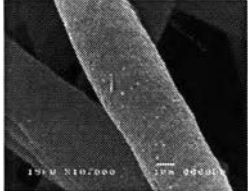
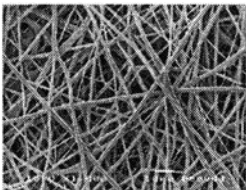
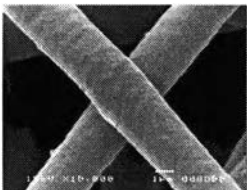
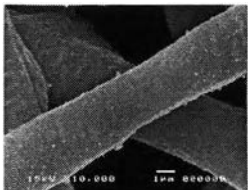
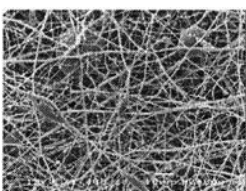
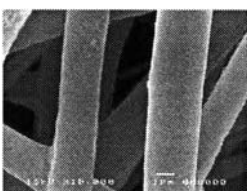
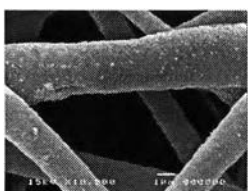


Figure 6.7 Indirect cytotoxicity evaluation of PHB-Fe₃O₄ composite nanofibers on the viability of mouse fibroblasts (L929) and murine neuroblastoma (Neuro2a) that were cultured with the extraction media from these materials for 1 d, 3 d and 5 d. The viability of the cells that were cultured with fresh culture medium (SFM) (i.e., control) was used as the reference to arrive at the viability of the attached cells shown in the figure.

Table 6.1 Selected SEM images of the as-spun pristine PHB, PHB containing iron ion and corresponding PHB-Fe₃O₄ composite nanofibers that were produced under a constant electrical potential of 15 kV and over a fixed collection distance about 20 cm.

Aqueous iron ion concentration (M)	Before ammonia treatment		After ammonia treatment Scale bar = 1 μ m Magnification = 10000x
	Scale bar = 10 μ m Magnification = 1000x	Scale bar = 1 μ m Magnification = 10000x	
Pristine PHB	 Fiber diameters: $2.68 \pm 0.79 \mu\text{m}$		 Particle size: no
0.05 M of aqueous iron ion	 Fiber diameters: $2.16 \pm 0.68 \mu\text{m}$		 Particle size: $67.62 \pm 15.40 \text{ nm}$
0.10 M of aqueous iron ion	 Fiber diameters: $1.31 \pm 0.53 \mu\text{m}$		 Particle size: $75.33 \pm 21.39 \text{ nm}$
0.20 M of aqueous iron ion	 Fiber diameters: $0.68 \pm 0.29 \mu\text{m}$		 Particle size: $82.81 \pm 25.74 \text{ nm}$